Aerosol Effects on Intensity of Landfalling Hurricanes as Seen from Simulations with the WRF Model with Spectral Bin Microphysics

A. KHAIN AND B. LYNN

Department of Atmospheric Sciences, The Hebrew University of Jerusalem, Jerusalem, Israel

J. DUDHIA

NCAR, Boulder, Colorado

(Manuscript received 3 June 2009, in final form 30 July 2009)

ABSTRACT

The evolution of a superhurricane (Katrina, August 2005) was simulated using the Weather Research and Forecasting Model (WRF; version 3.1) with explicit (nonparameterized) spectral bin microphysics (SBM). The new computationally efficient spectral bin microphysical scheme (FAST-SBM) implemented to the WRF calculates at each time step and in each grid point the size distributions of atmospheric aerosols, water drops, cloud ice (ice crystals and aggregates), and graupel/hail. The tropical cyclone (TC) evolution was simulated during 72 h, beginning with its bypassing the Florida coast (27 August 2005) to its landfall just east of New Orleans, Louisiana (near the end of 29 August). The WRF/SBM was used to investigate the potential impact of aerosols ingested into Katrina's circulation during its passage through the Gulf of Mexico on Katrina's structure and intensity. It is shown that continental aerosols invigorated convection largely at TC periphery, which led to its weakening prior to landfall. Maximum weakening took place ~24 h before landfall, just after its intensity had reached its maximum. The minimum pressure increased by ~15 hPa, and the maximum velocity decreased up to 15 m s^{-1}. Thus, the model results indicate the existence of another (in addition to a decrease in the surface fluxes) mechanism of weakening of TCs approaching the land. This mechanism is related to effects of continental aerosols involved in the TC circulation. It is shown that aerosols substantially affect the spatial distribution of cloudiness and hydrometeor contents. The evolution of lightning structure within the TC is calculated and compared with that in Katrina. The physical mechanisms of aerosol-induced TC weakening are discussed.

1. Introduction

a. Factors affecting TC intensity

Tropical cyclones (TCs) are known for their destructive power, particularly as they make landfall. TCs are often accompanied by extreme winds, storm surges, and torrential rainfall. The prediction of TC intensity represents a difficult task. Well-known factors affecting TC intensity are heat and moisture surface fluxes, which in turn are determined by the sea surface temperature (SST) and wind shear (e.g., Anthes 1982; Khain and Sutyrin 1983; Khain 1984; Emanuel 2005). The implementation of TC–ocean coupling into prognostic TC models led to a significant improvement in the forecast of TC intensity (Falkovich et al. 1995; Bender and Ginis 2000). The mechanisms mentioned above represent thermodynamic factors affecting the convection intensity (i.e., the availability of latent heat for release in cumulus clouds). During the past decade it was found that aerosols (including anthropogenic ones) substantially affect cloud microphysics and consequently the rate of latent heat release, the dynamics, and precipitation (see overviews by Levin and Cotton 2009; Khain et al. 2009; Rosenfeld et al. 2008). In particular, it was found that small aerosols invigorate tropical convection, increasing vertical velocities and cloud top heights of deep convective clouds (Khain et al. 2004, 2005, 2008b; Koren et al. 2005; Lynn et al. 2005a,b; Wang 2005; Lee et al. 2008; Khain 2009). Thus, aerosols affect cloud microphysics and dynamics.

Until recently the possible effects of aerosols on TC intensity did not attract the attention of investigators.

Corresponding author address: Prof. Alexander Khain, The Hebrew University of Jerusalem, Jerusalem 91904, Israel.
E-mail: khain@vms.huji.ac.il

DOI: 10.1175/2009JAS3210.1

This can be attributed to the lack of sophisticated microphysical schemes in most current TC models. Besides, both experimental and numerical investigations of cloud microphysics in TCs are quite limited. Microphysical observations in TCs are usually limited by the zones of the melting level (McFarquhar and Black 2004). The lack of knowledge of the microphysical structure of clouds in TCs led in the past to the failure of the hurricane mitigation project STORMFURY (Simpson and Malkus 1964; Willoughby et al. 1985) based on the hypothesis that TC weakening can be achieved by glaciogenic seeding of cloud tops at the periphery of the eyewall. It was hypothesized that there is usually a significant amount of supercooled water at high levels in the eyewall. More detailed analysis (Willoughby et al. 1985) showed that there was too little supercooled water and too much natural ice in these clouds (Black and Hallett 1986). Correspondingly, the cloud microphysical structure did not match the Storm Fury hypothesis (see Rosenfeld et al. 2007 and Khain et al. 2008a for details). A numerical study by Khain and Agrenich (1987) was probably one of the first ones in which a possible effect of the Saharan dust on the TC development via heating of polluted air by solar radiation was investigated using an axisymmetric TC model. Some observations indicating possible aerosol effects on TC development via their influence on the cloud microphysics of TC clouds have been performed recently by Jenkins et al. (2008) and Jenkins and Pratt (2008).

b. *Lightning and microphysical processes*

An indirect evidence of aerosol effects on TC intensity can be derived from enhanced lightning in TC. It is well known that lightning over the sea is a much rarer phenomenon than over the land (e.g., Williams and Satori 2004; Williams et al. 2005). Charge separation needed for lightning formation is a result of collisions between low-density ice crystals with high-density graupel in the presence of a significant amount of supercooled water at temperatures below −13°C (e.g., Takahashi 1978; Saunders 1993; Black et al. 1996; Black and Hallett 1999; Cecil et al. 2002; Cecil and Zipser 2002; Sherwood et al. 2006; Betz et al. 2008). Such microphysical structure is not typical of maritime convection in clean air where efficient drop collisions below freezing level lead to the formation of raindrops falling down without freezing (warm rain). As a result, maritime clouds contain usually very low amounts of supercooled water. Thus, the formation of intense lightning in a TC indicates substantial changes in the cloud microphysical structure as compared to that of clouds in TC surroundings. Note that enhanced lightning intensity over the oceans takes place downwind of continents. It is reasonable to hypothesize that this increase in lightning takes place in zones of aerosol intrusion from continents. An increase in lightning rate indicates invigoration of convection (stronger updrafts with increasingly larger volumes of graupel or small hail/frozen drops aloft) and an increase in the probability of heavier rainfall (e.g., Lhermitte and Krehbiel 1979; Wiens et al. 2005; Fierro et al. 2007). The presence of lightning activity in storms crossing the West African coast can be used as a precursor to TC formation (Chronis et al. 2007). The appearance and intensification of lightning in the eyewall can be a predictor of TC intensification (Lyons and Keen 1994; Orville and Coyne 1999; Molinari et al. 1999; Shao et al. 2005; Demetriades and Holle 2006; Fierro et al. 2007; Price et al. 2009). Rodgers et al. (2000) found that the closer the lightning is to the storm center, the more likely the TC is to intensify. Molinari et al. (1994, 1999) analyzed the radial distribution of lightning in hurricanes approaching the U.S. coast using National Lightning Detection Network data. They found three zones of distinct electrical characteristics: (a) the inner core, which contains a weak maximum of flash density; (b) the region with a well-defined minimum in flash density extending 80–100 km outside this maximum; and (c) the outer band region, which contains a strong maximum of the flash density within the 200–300-km-radius ring around the hurricane center. The lightning activity in Hurricane Katrina (2005) at several successive time instances was presented by Shao et al. (2005). An analysis of the location of lightning within the zone of Katrina indicates that the appearance of strong lightning in the eyewall of Katrina was a precursor of the TC deepening, whereas the disappearance of lightning in the TC center and appearance of intense lightning at the TC periphery was the precursor of TC weakening (Fig. 1). Usually, enhanced lightning at the TC periphery is attributed to atmospheric instability (e.g., Molinari et al. 1994, 1999).

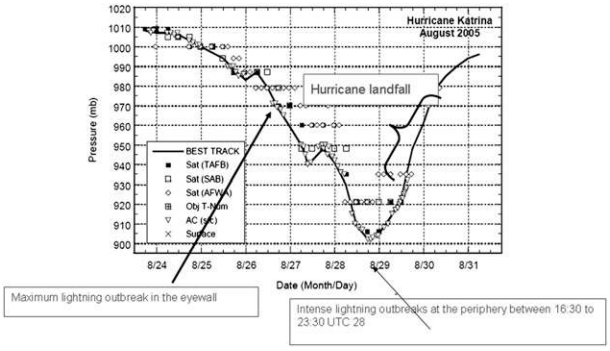

FIG. 1. Minimum pressure in Hurricane Katrina. Maximum lightning intensity in the eyewall takes place before rapid intensification of the hurricane, whereas maximum lightning at the TC periphery is a precursor of TC weakening.

Lightning in the TC eyewall is often attributed to instabilities that result in ''convective bombs'' or explosive convection in the eyewall that produces the large updrafts and conditions suitable for lightning. Khain et al. (2008a) analyzed the mechanisms of lightning formation in Katrina (as well as in other landfalling hurricanes) in more detail. They showed that a penetration of continental aerosols to clouds at the TC periphery and successive convection invigoration is the mechanism contributing substantially to lightning formation at the TC periphery. An increase in concentration of small aerosols increases droplet concentration and decreases droplet size. The net effect is the decrease in the collision rate, delay in raindrop formation, and warm rain production. As a result, small droplets ascend in cloud updrafts and continue growing by condensation. It leads to an increase in supercooled water content, which intensifies the riming (i.e., ice–water collisions accompanied by freezing of liquid water). Both processes (diffusion drop growth and freezing by riming) are accompanied by extra latent heat release, leading to an increase in cloud updrafts and sometimes to an increase in cloud-top height (see overview by Khain 2009). Aerosol-induced increase in supercooled cloud water content (CWC) and vertical velocities foster the formation of conditions favorable for charge separation and lightning formation, when collisions of ice crystals and graupel take place in the presence of supercooled droplets.

c. *Modeling with microphysical treatment*

Khain et al. (2008a) simulated the evolution of Hurricane Katrina (August 2005) during its movement in the Gulf of Mexico using the Weather Research and Forecasting (WRF) Model [National Center for Atmospheric Research (NCAR) version] with two nested grids. The resolutions of the finest and of the outer grid were 3 and 9 km, respectively. The Thompson et al. (2006) one-moment bulk parameterization was used to describe microphysical processes in clouds and the corresponding latent heat release. Parameters determining autoconversion rate were calculated in this scheme by presetting the droplet concentration. Supplemental simulations with droplet concentration varying from 100 to 1000 cm^{-3} showed, however, that the scheme is not sensitive to the aerosol concentration. To sidestep this problem, Khain et al. (2008a) simulated the effects of continental aerosols by preventing warm rain in the scheme altogether by shutting off the drop–drop collisions only at the hurricane periphery. A similar approach was used by Rosenfeld et al. (2007). The results obtained in these idealized simulations led to an increase in supercooled water and ice contents in the rainbands at the TC periphery and allowed Khain et al. (2008a) to conclude that continental aerosols that penetrated the TC periphery caused enhanced lightning flashes in the areas of penetration. It was also shown that aerosols, invigorating clouds at 250–300 km from the TC center, decrease the convection intensity in the TC eyewall, leading to some TC weakening. Similar results were reported by Rosenfeld et al. (2007), who proposed a method of TC mitigation by seeding of clouds at the TC periphery near their cloud base with small aerosol particles of 0.05 to 0.1 μm in radius.

Simulations of the evolution of an idealized TC using the Regional Atmospheric Meteorological System (RAMS; Zhang et al. 2007) supported the conclusion that aerosols (e.g., Saharan dust) can substantially affect the intensity of TCs.

To properly take into account microphysical factors (such as aerosols), advanced microphysical schemes are required. At the same time, the problem of the adequate description of convection in TC models remains one of the most difficult problems in TC modeling and forecasting. The current operational TC forecast model developed at the Geophysical Fluid Dynamics Laboratory (GFDL) used large-scale convective parameterizations until 2006 (Kurihara 1973; Arakawa and Shubert 1974). Since 2006 this model has used a simplified Arakawa–Schubert scheme for its cumulus parameterization, and a simplified version of the Ferrier bulk parameterization (Ferrier 2005) to calculate large-scale condensation under conditions of supersaturation (Bender et al. 2007). The simplified bulk scheme treats only the sum of the hydrometeor classes (referred as the total condensate) in the advection in both horizontal and vertical direction. Both schemes are insensitive to aerosols.

The development of one- and two-moment bulk parameterization schemes and their application in mesoscale models such as the fifth-generation Pennsylvania State University–NCAR Mesoscale Model (MM5; Dudhia et al. 1993), the Regional Atmospheric Modeling System (RAMS; Pielke et al. 1992), the WRF model (Skamarock et al. 2005), and the operational numerical weather prediction model of the German Weather Service (COSMO) combined with an extended version of the two-moment bulk scheme by Seifert and Beheng (2006), etc., was an important step toward the improvement in the description of convective processes and precipitation in numerical models. A priori prescription of the shape of size distribution functions of different cloud hydrometeors (e.g., cloud droplets, rain drops, graupel, aggregates) in the form of exponential Marshall–Palmer distributions or gamma distributions reduces the system of equations that describes cloud microphysics to a relatively small number of equations for integral quantities such as mass contents (one-moment schemes) and mass contents and

concentrations (two-moment schemes). The comparatively small number of prognostic equations makes the schemes computationally efficient, so they are widely utilized in simulating different cloud-related phenomena such as supercell storms and squall lines. Recently these schemes were used for simulation of TCs (e.g., Zhang et al. 2007; Fierro et al. 2007).

The bulk parameterization schemes, especially one-moment schemes, have substantial limitations in describing microphysical processes affecting the shape of size distributions (such as aerosol effects). Besides, these schemes as a rule do not solve the equation for diffusion growth of drops (this equation is replaced by transformation of all supersaturated water vapor into cloud water mass, so that the final supersaturation is assumed equal to zero). Instead of solving the stochastic equation of collisions, all one-moment and most two-moment bulk schemes use semiempirical relationships for autoconversion rates, often with hidden or internal assumptions about cloud droplet number concentrations. A substantial shortcoming of most bulk schemes is utilization of a single settling velocity and single collision efficiency for an entire distribution of cloud droplets and given ice species.[1]

The second approach to simulate microphysical processes is the utilization of spectral bin microphysics (SBM), in which a system of kinetic equations for size distributions of particles of different classes is solved. Each size distribution function is described using several tens of mass (size) bins. The equation system solves the equations for advection, settling, collisions, freezing, melting, and so on for each mass bin (each particle size). The SBM describes aerosol effects on cloud microphysics and dynamics taking into account the aerosol budget (i.e., a limited source of aerosol particles). This method is much more accurate than the bulk parameterization with regard to its ability to simulate cloud dynamics and microphysics and precipitation (see comparisons of SBM versus bulk schemes in Lynn et al. 2005b; Lynn and Khain 2007; Li et al. 2009a,b; Iguchi et al. 2008; Khain and Lynn 2009; Khain et al. 2009). As mentioned by Khain et al. (2008a), the utilization of high-resolution TC models with SBM could grant greater credibility to simulations of TC and the effects of aerosols on TCs. However, the basic SBM scheme described by Khain et al. (2004, 2008b) requires ~50 times more computer time than standard one-moment bulk parameterization schemes, which hinders their wide application in mesoscale models, particularly in TC models.

In this study the evolution of Hurricane Katrina over the Gulf of Mexico is simulated with WRF, in which cloud microphysics is described using a computationally efficient spectral bin microphysics scheme, with all microphysical processes described explicitly.

2. Model and experimental design

a. Spectral bin microphysics scheme

The SBM scheme implemented into the WRF (version 3; Skamarock et al. 2005) has been described by Khain et al. (2004) and Lynn and Khain (2007). The scheme is based on solving the kinetic equation system for the size distributions of seven classes of hydrometeors: water drops, three types of crystals (columnar, plate, and branch types), aggregates (snow), graupel, and hail. Each hydrometeor class is described by a size distribution function defined on the grid of mass (size) containing 33 mass bins. A doubling mass grid is used, so that the mass of drops belonging to the $(i + 1)$th bin is twice as large as the drop mass in the ith bin. The mass grids are similar for all hydrometeors to simplify the transition from one type to another during freezing, melting, etc. The minimum particle mass corresponds to that of the 2-μm-radius droplet. The model is specially designed to take into account aerosol effects on cloud microphysics. It contains an aerosol budget, which describes two-way cloud–aerosol interaction. Aerosol particles are also described by a size distribution function containing 33 size bins. In contrast to the standard bulk parameterization schemes, the size distributions of cloud hydrometeors and aerosols are not prescribed a priori but rather are calculated in the course of the model integration. Supersaturation is calculated using an accurate analytical method (Khain et al. 2008b) representing an extension of the approaches developed earlier by Tzivion et al. (1989) and Khain and Sednev (1996). Using the values of supersaturation, the critical size of aerosol particles to be activated to drops is calculated. Aerosol particles exceeding the critical size are activated and the corresponding mass bins in the aerosol size distribution become empty. It means that within the cloud updraft we have two fluxes: the flux of droplets and the flux of nonactivated cloud condensation nuclei (CCN). When supersaturation exceeds its local maximum at the cloud base, a new portion of CCN will be activated to droplets (in-cloud nucleation). This process is especially

[1] Modification of bulk parameterization schemes is usually related to the implementation of bin-mimic procedures—keeping, however, the shape of size distributions prescribed a priori. The most advanced bulk scheme used in RAMS includes bin-mimic procedures of hydrometeor settling, collisions (riming), drop nucleation, and some other procedures. It uses a two-mode distribution of cloud droplets that better represents the full drop spectrum. It allows utilization of RAMS for investigation of aerosol effects in many cloud-related phenomena. Recent versions of the scheme are described in detail by Saleeby and Cotton (2004, 2008).

important in maritime clouds where supersaturation is high and often increases with height because of a decrease in droplet concentration and increase in vertical velocity with height. The inclusion of this process leads to the formation of bimodal droplet spectra with realistic droplet spectra dispersion (Pinsky and Khain 2002; Segal and Khain 2006; Segal et al. 2003). The SBM also takes into account possible droplet nucleation during dry air entrainment through the lateral cloud boundaries.

A new approach has been applied to eliminate artificial spectrum broadening typical of previous spectral microphysical schemes (including the earlier version of this model; see Khain et al. 2000). In this method, the remapping of size distribution functions obtained after diffusion growth to the regular mass grid conserves the three moments of size distribution (zeroth, third, and sixth moments) to prevent artificial formation of large-sized tails in the drop distribution (Khain et al. 2008b). This approach allows the formation of very narrow droplet spectra found in smoky and pyro-clouds measured during biomass burning over Brazil (Andreae et al. 2004). Note that in the SBM, water drops are not separated artificially into cloud water and rainwater (in contrast to in all bulk-parameterization schemes). It means that the SBM does not separate the collision process of water drops into accretion (collisions of cloud droplets) and collection (collisions of rain drops and cloud droplets), which is performed in all bulk schemes under the simplification of continuous growth. Instead, in SBM the cloud particle collisions are calculated by solving the stochastic kinetic equations for collisions. An efficient and accurate method of solving the stochastic kinetic equation for collisions (Bott 1998) was extended to a system of stochastic kinetic equations calculating water–ice and ice–ice collisions. The collision kernels for each pair of particles are calculated using an accurate superposition method (Pinsky et al. 2001; Khain et al. 2001a) and used in the form of lookup tables. The collision kernels are calculated taking into account the particle shape and density that are represented as the functions of particles mass following Pruppacher and Klett (1997) (see Khain and Sednev 1996; Khain et al. 2004 for details). The ice nuclei activation is described using an empirical expression suggested by Meyers et al. (1992) and applying a semi-Lagrangian approach (Khain et al. 2000) to allow the utilization of the proposed diagnostic formulas in a time-dependent framework. Secondary ice generation is described according to Hallett and Mossop (1974). The rate of drop freezing follows the observations of immersion nuclei by Vali (1975, 1994) and homogeneous freezing according to Pruppacher (1995). Breakup of raindrops is described following Seifert et al. (2005).

The SBM model does not requires any tuning of the scheme parameters and was successfully used without any changes for simulation of deep maritime convection (Khain et al. 2004, 2008b), continental clouds including pyro-clouds (Khain et al. 2001b, 2008b), squall lines (Lynn et al. 2005a,b; Tao et al. 2007; Li et al. 2009a,b; Khain et al. 2009), supercell storms (Khain and Lynn 2009), and Arctic stratiform clouds (Fan et al. 2009).

Note that the treatment of eight size distributions (advection of all bins, with collisions between particles belonging to different bins) requires a significant computer time, which is about 50 times longer than that required by a standard one-moment bulk parameterization scheme (in a three-dimensional simulation).

To reduce computer time, a Fast-SBM has been developed and applied in the study. In the Fast-SBM all ice crystals and snow (aggregates) are calculated on one mass grid (one distribution function). The smallest ice particles with sizes below 150 μm are assumed to be crystals, while larger particles are assigned to aggregates (snow). Similarly, high-density particles (graupel and hail) are also combined into one size distribution (graupel). No changes in the description of microphysical processes compared to the Full-SBM have been made. As a result, the number of size distributions decreases from eight to four (aerosols, water drops, low-density ice, high-density ice). Note that Fast-SBM keeps the main advantages of SBM: a kinetic equation system is solved using the nonparameterized basic equations, particles of each size have their own settling velocity, particles depending on their mass have different densities, etc. The test simulations showed that Fast-SBM requires less than 20% of the time of the full SBM, which makes it possible to use the Fast-SBM on standard PC clusters.

The detailed comparison of results obtained by the Full and Fast SBM was described by Khain et al. (2009), where a tropical squall line was simulated using both SBM schemes. It was shown that the Fast SBM produces the microphysical and dynamical structure of the squall line as well as accumulated rain at the surface quite similar to those simulated with Full SBM. We suppose that for the simulation of tropical maritime deep convection it is not so important to reproduce many types of ice crystals, as well as specific properties of hail, because deep maritime clouds contain comparatively small amount of such hydrometeors.

b. Experimental design

A set of simulations were used to study possible aerosol effects on the evolution of Hurricane Katrina (August 2005) in the Gulf of Mexico during about three days (beginning at 0000 UTC 27 August) prior to and including landfall (on about 1200 UTC 29 August). A

two-nested gridded WRF (version 3.1) was used, and the nest moved using a cyclone-following algorithm. The resolutions of the finest and of the outer grid were 3 and 9 km, respectively. The number of the vertical levels was 31, with the distances between the levels increasing with the height. The SBM is applied at the finest grid of size 400 km × 400 km; on the outer grid, the bulk parameterization of Thompson et al. (2006) was used. Integral parameters of clouds (mass contents) penetrating from the outer grid into the fine grid were recalculated into size distribution functions assuming a Marshall–Palmer size distribution as defined in the bulk parameterization scheme. If clouds formed in the internal area penetrated the outermost grid, the size distribution functions of hydrometeors in these clouds are used to calculate mass contents used by the bulk parameterization.

The initial fields were taken from the Global Forecast System Reanalysis data. The lateral boundary conditions were updated every 6 h using the data as well. The Gulf of Mexico surface water temperature was initialized at 0000 UTC 27 August and was not updated during the experiments. According to the reanalysis data the SST taken along the TC track reached its maximum near the shore (the place of the TC landfall).

Cloud droplets arise on aerosol particles (AP) playing the role of cloud condensation nuclei (CCN). The initial (at $t = 0$) CCN size distribution is calculated using the empirical dependence of concentration of activated CCN N_{CCN} on supersaturation with respect to water S_w (in %):

$$N_{\mathrm{CCN}} = N_o S_w^k, \tag{1}$$

where N_o and k are the measured constants for determining the AP concentration and shape of the AP size distribution, respectively.

This method for calculating initial AP size distribution is based on the Kohler theory and described by Khain et al. (2000) in detail. At $t > 0$ the prognostic equation for the size distribution of nonactivated AP is solved. The initial AP concentration was assumed constant within the lowest 2-km layer and decreased exponentially with height with characteristic scale of 2 km. Aerosols were transported over the entire computational area similarly to other scalars like the mixing ratio.

To investigate aerosol effects on microphysics and the dynamics of the TC two simulations were carried out: 1) in the first simulation (hereafter MAR) N_o was set equal to 100 cm^{-3}, typical of maritime atmosphere over the whole computational area; 2) in the second, semicontinental case (hereafter MAR_CON) the initial CCN concentration over the land N_o was set equal to 1500 cm^{-3}, typical of continents under not very polluted conditions. Initially, over the sea N_o was set equal to 100 cm^{-3} in all simulations. In all simulations the slope parameter k was set equal to 0.5. When the TC entered the Gulf of Mexico, its circulation transported aerosols from the land to sea, so that some continental aerosols penetrate clouds within the TC and affect their microphysics and dynamics. The impact of continuing emissions was taken into account by continuing a flux of aerosols into the boundaries of the coarse domain. In all simulations the maximum size of dry AP was equal to 2 μm, which gave rise to droplets of radius 8 μm at cloud base. No giant CCN that could arise at high winds as a result of spray formation were assumed in the simulations. The role of CCN with sizes of 2 μm was investigated in detail by Khain et al. (2008a). It was shown that in the presence of large concentrations of small aerosols, concentration of droplets is high and supersaturation is low. As a result, droplets forming on large CCN grow slowly and do not affect substantially the microphysical and dynamical structure of clouds. The role of giant CCN may be significant in the central zone of TC and will be investigated in a future study.

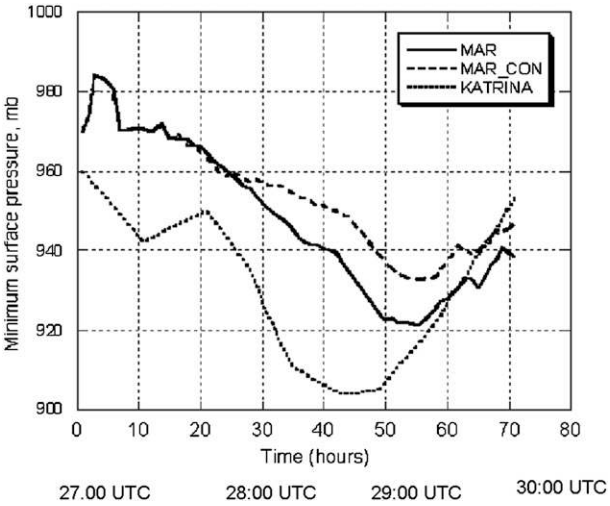

FIG. 2. Time dependence of minimum pressure in numerical experiments and Hurricane Katrina (August 2005).

Note that there are some uncertainties with regard to the concentration and size distributions of continental AP that may form over the land under strong winds. A concentration of 3000 cm^{-3} (instead of 1500 cm^{-3} used) seems also to be realistic. In this sense our simulations can be considered as a sensitivity study of TCs to continental aerosols involved in TC circulation.

3. Results of simulations

a. Effects of aerosols on minimum pressure in TC

Figure 2 shows the time dependence of minimum pressure in all simulations and in Katrina. One can see

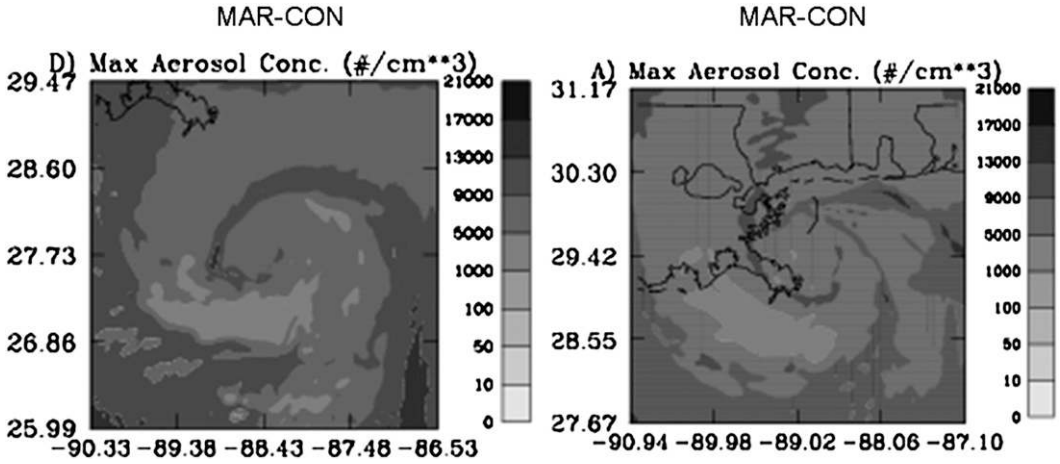

FIG. 3. Fields of maximum AP concentration in the MAR_CON simulation at (left) 2300 UTC 28 Aug and (right) 0900 UTC 29 Aug on the fine grid.

that the modeled TC had lower intensity during the first ~50 h of simulations as compared to that of Katrina. Note in this connection that the WRF model used did not have specific adjustment procedures typically used in the TC forecast models to adopt the TC structure. In our case the initial data were derived from the crude-resolution (100 km) reanalysis data at $t = 0$ (0000 UTC 27 August). Hence, some relaxation period was required to get the model TC intensity close to the observed one. However, the accurate prediction of the Katrina's intensity was not the primary purpose of the study. The main purpose of the simulations was to compare the TC intensity and structure in the simulations with and without aerosol effects on the TC clouds in a strong

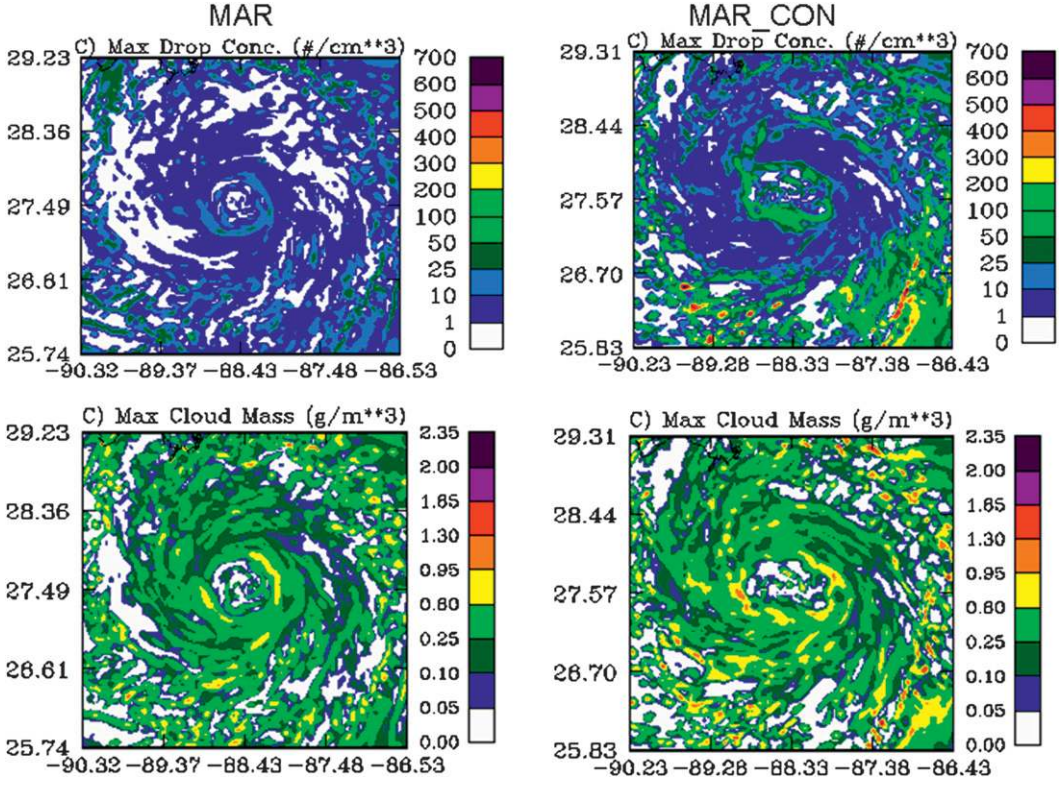

FIG. 4. Fields of (top) maximum droplet concentrations and (bottom) CWC in simulations (left) MAR and (right) MAR-CON at 2200 UTC 28 Aug at the fine grid.

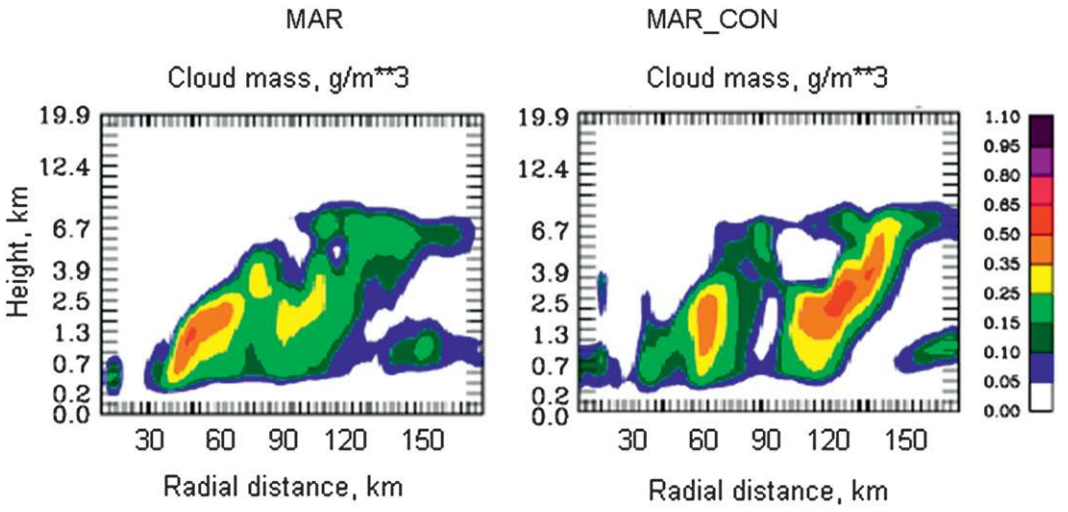

FIG. 5. The cross section of azimuthally averaged CWC in simulations (left) MAR and (right) MAR-CON at times when the maximum difference in the TC intensities took place.

hurricane, which is able to ingest aerosols from the continent. Figure 2 shows that TC in the MAR_CON run turned out substantially weaker, so that at the time instances when the TC reached its maximum intensity the minimum pressure in its center was about ~15 hPa higher than in the MAR run. Note that lower (as compared to Katrina) intensity of the model TC leads likely to an underestimation of aerosol effects because a weaker

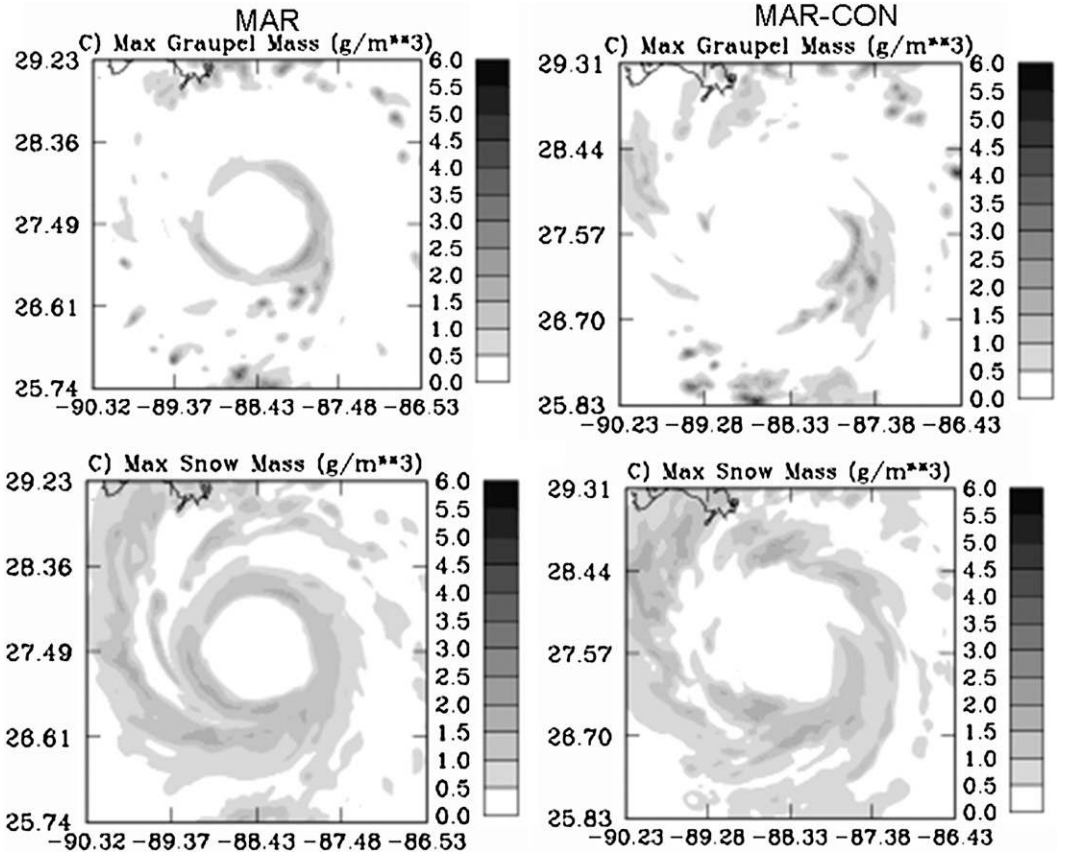

FIG. 6. As in Fig. 4, but for fields of (top) graupel and (bottom) snow contents.

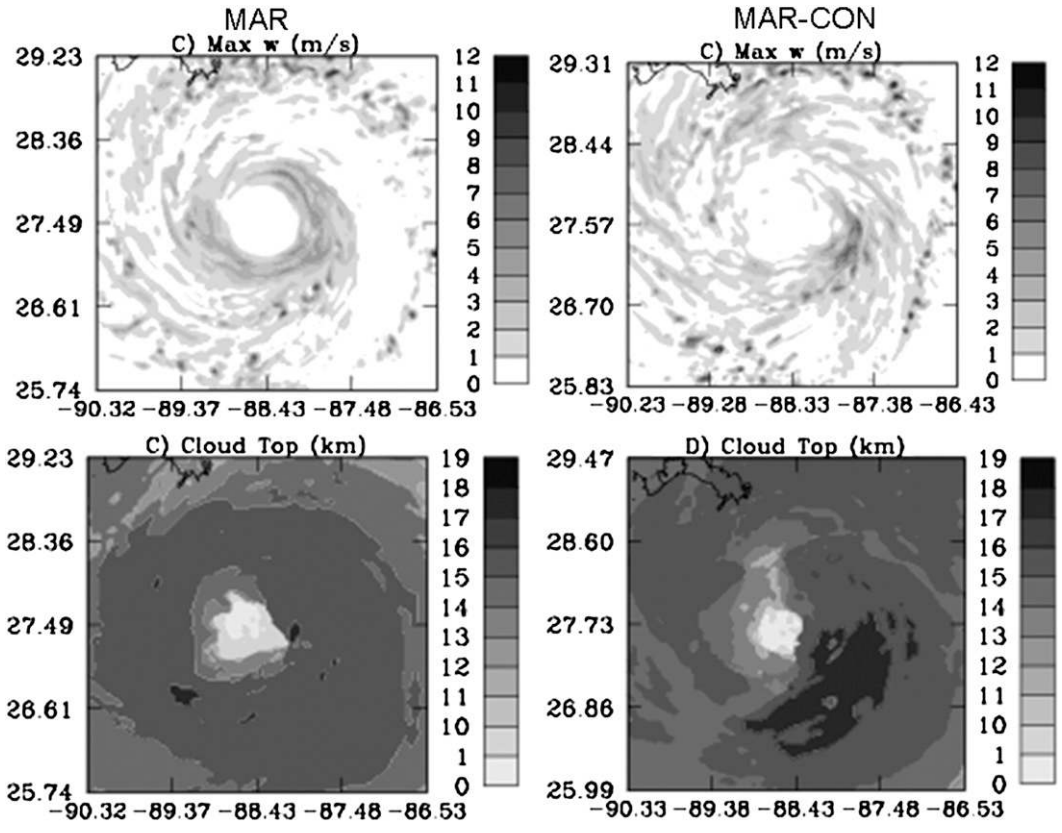

FIG. 7. As in Fig. 4, but for fields of (top) vertical velocity and (bottom) cloud-top height.

TC transports lower AP amounts into the TC circulation. The results shown in Fig. 2 indicate that aerosol effects are an important factor affecting the TC intensity.

b. Aerosol effect on microphysical and dynamical fields

In the analysis of the aerosol fields we addressed two main questions. The first one was whether a significant aerosol concentration can enter the TC periphery when it is located at comparatively large distance from the coast line; the second is whether aerosols can penetrate the TC eye. Aerosol fields simulated in the MAR run (not shown) indicate a very uniform distribution of AP concentration (which is very low) because the AP concentration over land was assumed equal to that over the sea. Figure 3 shows the fields of the AP concentration maximum in MAR_CON at (left) 2300 UTC 28 August and (right) 0900 UTC 29 August on the fine grid. The analysis of Fig. 3 shows that (a) the AP concentration at the TC periphery approached concentrations similar to those over the continent; (b) over a significant area the aerosol concentration decreased while approaching the TC center, partially because of the activation of aerosols to cloud droplets (nucleation scavenging); and (c) aerosols can penetrate the TC eyewall clouds along comparatively narrow streams.

Note that the concentration of AP in the AP size distribution is much higher than N_o in (1). The value of N_o indicates the number of AP activated at supersaturation of 1%. The minimum size of soluble aerosol particles activated at this supersaturation is about 0.01 μm. The aerosol size distribution used in the simulations contained a significant amount of smaller AP. In the model we did not take into account aerosol scavenging by washout. The decrease in aerosol concentration is caused by the nucleation scavenging the droplet activation and by their fall to the surface. Nevertheless, we suppose that a significant amount of smallest AP can reach the eyewall in real TCs because of very low collection efficiency between rain drops and AP with sizes below 0.01 μm.

The analysis of the aerosol concentration fields during the TC evolution indicates that AP reach clouds at the TC periphery at about 2000 UTC 27 August, but a substantial decrease in the TC intensity (measured by the minimum pressure or the maximum value of wind speed) began only at $t > 30$ h (Fig. 2); that is, the intensity of the TC responded to the changes in convection with a delay

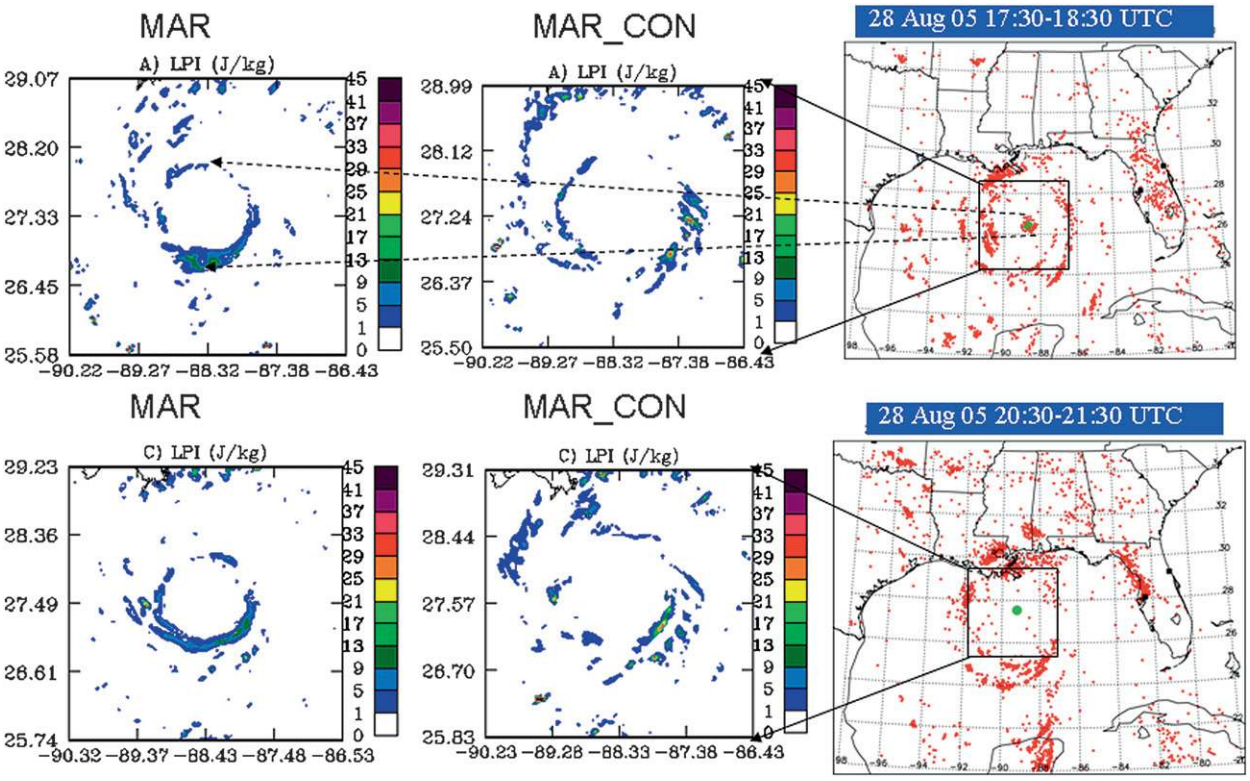

FIG. 8. The fields of LPI calculated in MAR and MAR-CON runs at 2000 and 2200 UTC 28 Aug. The lightning in Katrina (2005) is also presented (after Shao et al. 2005). Zones of lightning are marked by red dots; the TC eye is marked green. The square shows the location of the fine grid approximately corresponding to these time instances.

of about 10 h. Note that a delay of similar duration was found between the intensification of lightning in the TC center and TC intensification (Price et al. 2009). Such a delay is related to TC inertia: several hours are needed for beginning of TC intensity to response to convection intensification, change in SST, and other factors (see, e.g., Khain and Sutyrin 1983; Khain 1984).

Because of some differences in the TC behavior on 28 August, when it was located comparatively far from the land, and on 29 August, when the TC landfall took place, we will analyze the microphysical and dynamical fields simulated during these days separately. Figure 4 compares the fields of the (top) column-maximum droplet concentrations and (bottom) cloud water mass content (clouds with radii below 40 μm) in clouds in simulations (left) MAR and (right) MAR-CON at 2200 UTC August 28 on the fine grid (46 h; Fig. 2). One can see that in the MAR run the droplet concentration does not exceed 50–100 cm^{-3}, which is a typical droplet concentration in clouds arising in clean maritime air. Zones of maximum droplet concentration in the MAR run at the TC periphery indicate zones of higher vertical velocities in rainbands. In MAR-CON, the penetration of continental aerosols led to an increase in droplet concentration at the TC periphery in the zone of high aerosol concentration, as well as in the eyewall. In the MAR-CON run the maximum droplet concentration reached 500 cm^{-3} (especially high concentrations are at the TC periphery), which is substantially higher than those in typical maritime clouds. An increase in droplet concentration within the eyewall in the MAR-CON run indicated that aerosols penetrated to the TC eyewall in the simulations.

The CWC dramatically increased (mainly supercooled water content) as a result of aerosol penetration: while the maximum CWC reached 0.6 g m^{-3} in the MAR run, the CWC in the MAR-CON run exceeded 1.6 g m^{-3}. The CWC increased largely at the TC periphery where concentration of aerosols was higher. To illustrate the difference in the structure of CWC in MAR and MAR_CON, Fig. 5 shows the cross section of azimuthally averaged CWC in these runs at the time instance when the maximum difference in the TC intensities took place. One can see that whereas small droplets in MAR reach about 3.5 km and produce warm rain, small droplets in MAR-CON reach ~8 km, indicating the formation of a high amount of supercooled water. One can see that aerosols led also to an increase in the radius of the eyewall, which usually indicates TC weakening.

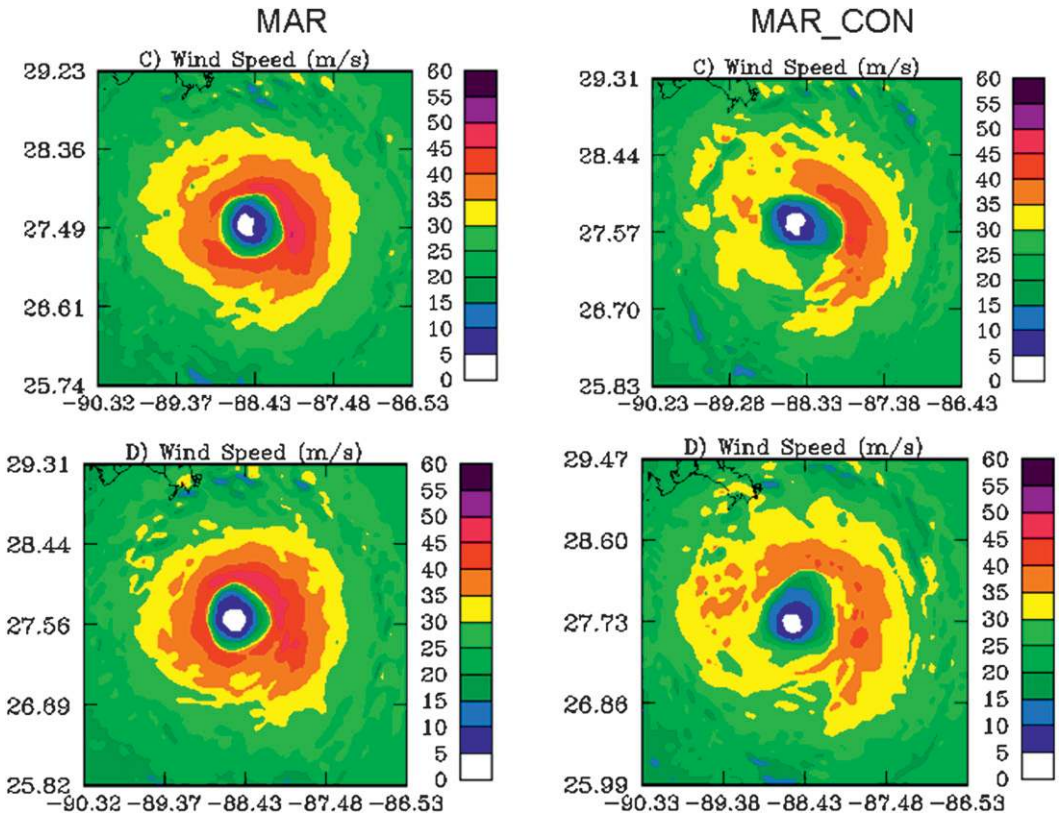

FIG. 9. The fields of maximum wind speed at (top) 2100 and (bottom) 2200 UTC 28 Aug in (left) MAR and (right) MAR_CON.

The aerosol-induced changes in warm microphysics resulted in corresponding changes in ice microphysics. The penetration of larger amounts of drops above the freezing level led to an increase in graupel and snow (aggregate) contents at the TC periphery (Fig. 6). Note that convection invigoration of clouds at the TC periphery weakened the updrafts in the eyewall, which immediately resulted in the decrease and even disappearance of graupel and snow in the eyewall. Extra latent heat release caused by droplet condensation and freezing in the periphery caused an increase in vertical updraft velocities and cloud-top height (Fig. 7). The values of maximum vertical velocities exceed 10 m s^{-1}, which is a quite rare situation for maritime TC clouds (Jorgensen et al. 1985; Jorgensen and LeMone 1989). At the same time, such high velocities are required to form lightning. The increase in cloud-top height within polluted air was observed from satellites (Koren et al. 2005) and simulated in many recent studies dedicated to aerosol effects on cloud dynamics (see review by Khain 2009).

c. *Aerosol effects on lightning in TC*

As discussed above, Khain et al. (2008a) suggested that the evolution of lightning within a TC approaching the land results from the ingestion of continental aerosols into the TC periphery. The present study strongly supports this finding. For instance, Fig. 8 presents the fields of the lightning potential index (LPI) at 2000 and 2200 UTC 28 August ($t = 44$ and 46 h in Fig. 2). The LPI was introduced by Yair et al. (2009) and Lynn and Yair (2009, manuscript submitted to *Adv. Geophys.*). The LPI is the volume integral of the total mass flux of ice and liquid water within the ''charging zone'' (0° to −20°C) of the cloud. It is calculated using the simulated grid-scale vertical velocity and simulated hydrometeor mass mixing ratios of liquid water, cloud ice, snow, and graupel as $\mathrm{LPI} = 1/V \iiint \varepsilon w^2 \, dx \, dy \, dz$, where V is the model unit volume and w is the vertical wind component in m s^{-1}. In essence, ε is a scaling factor for the cloud updraft and attains a maximal value when the mixing ratios of supercooled liquid water and of the combined ice species (the total of cloud ice, graupel, and snow) are equal. It signifies the fact that charge separation requires all these ingredients to operate synergistically within the charging zone, as shown by many laboratory experiments summarized by Saunders (1993). The LPI has the same meaning as the lightning probability parameter introduced by Khain et al. (2008a). Figure 8 shows also

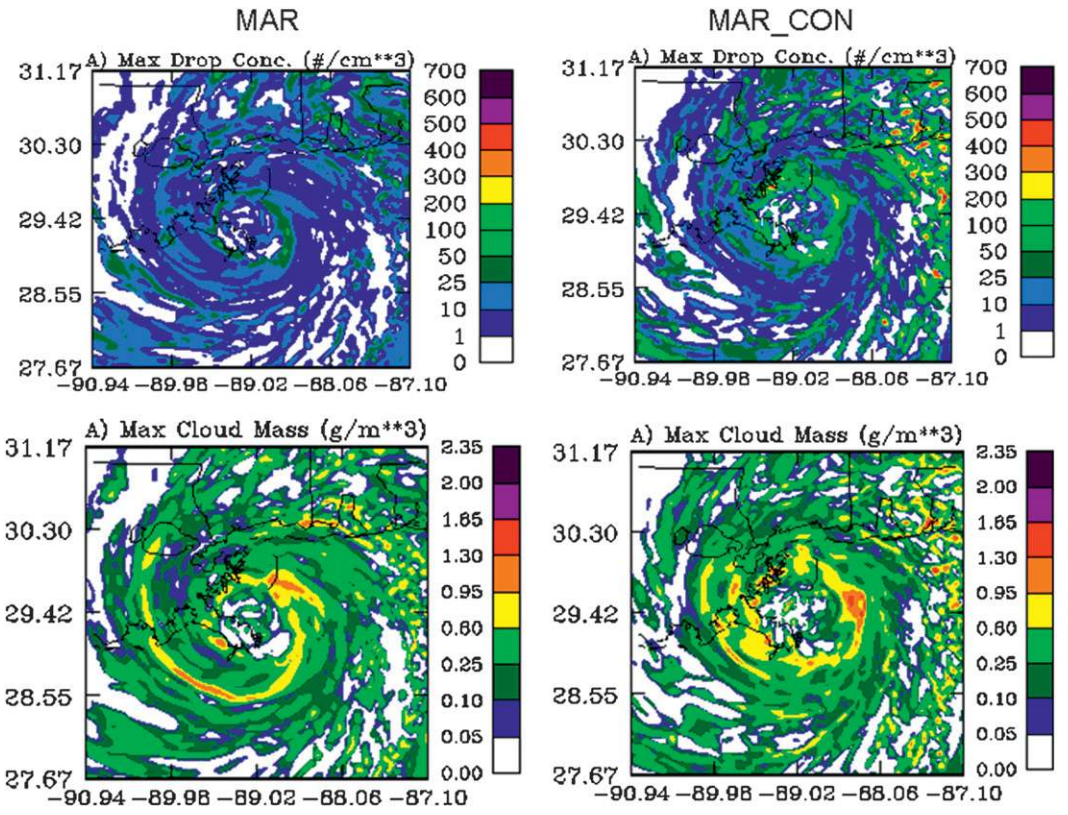

FIG. 10. As in Fig. 4, but for 0900 UTC 29 Aug.

lightning in Katrina (2005) at two different time instances (Shao et al. 2005). The squares show the location of the fine grid approximately corresponding to these time instances. One can see that in the MAR run the LPI is the highest in the eyewall all the time, independent of the distance from the land. Note that simulations of lightning in TC using bulk parameterization schemes (Fierro et al. 2007) (in which aerosol effects were not taken into account) also indicate that lightning was concentrated in the TC central area independent of the stage of TC evolution.

At $t < 40$ h, lightning is intense in the TC eyewalls in both runs; however, in the MAR_CON run a new ring of lightning at radii of 150–180 km arises at $t \sim 30$ h, continuously intensifies with time, and becomes dominant at $t > 46$ h. Figure 8 shows the time instance of the dissipation of the internal lightning ring in the course of intensification of convection and lightning at the TC periphery. One can see that the disappearance of lightning in the eyewall in MAR-CON run agrees well with the behavior of lightning in Katrina. The disappearance of lightning in the eyewall in MAR-CON takes place about 5–6 h before the TC weakening. We see therefore that the decrease in lightning in the TC center and its increase at the TC periphery can serve as a precursor of TC weakening.

Figure 9 shows the fields of maximum wind speed at (top) 2100 and (bottom) 2200 UTC 28 August in MAR and MAR_CON. One can see a significant decrease in the maximum wind speed up to 15 m s^{-1} (i.e., by 20%–25%). This decrease is substantially stronger than reported by Khain et al. (2008a), which can be attributed to utilization of SBM.

Several figures illustrate the changes of TC structure during landfall. Figures 10–12 show fields similar to those in Figs. 4, 6, and 7, respectively, but for 0900 UTC 29 August, when the simulated TC was quite close to the land. Again, we see that aerosols increase droplet concentration and CWC. Note that the TC in MAR-CON is weaker than that in MAR, with a much weaker eyewall; the eyewall has larger radius (see Figs. 10 and 11) and lower cloud-top height (Fig. 12). Figure 13 shows fields of the maximum wind speeds in the (left) MAR and (right) MAR_CON runs at the same time instances of 0900, 1100, and 1200 UTC. One can see that the maximum wind speed in MAR-CON is substantially lower than in MAR. In addition, the area of strong wind is also substantially lower in MAR-CON. Note the existence of a sharp decrease in the maximum wind speed over the land. We attribute this decrease to the effect of surface friction. These figures indicate that the aerosol-induced

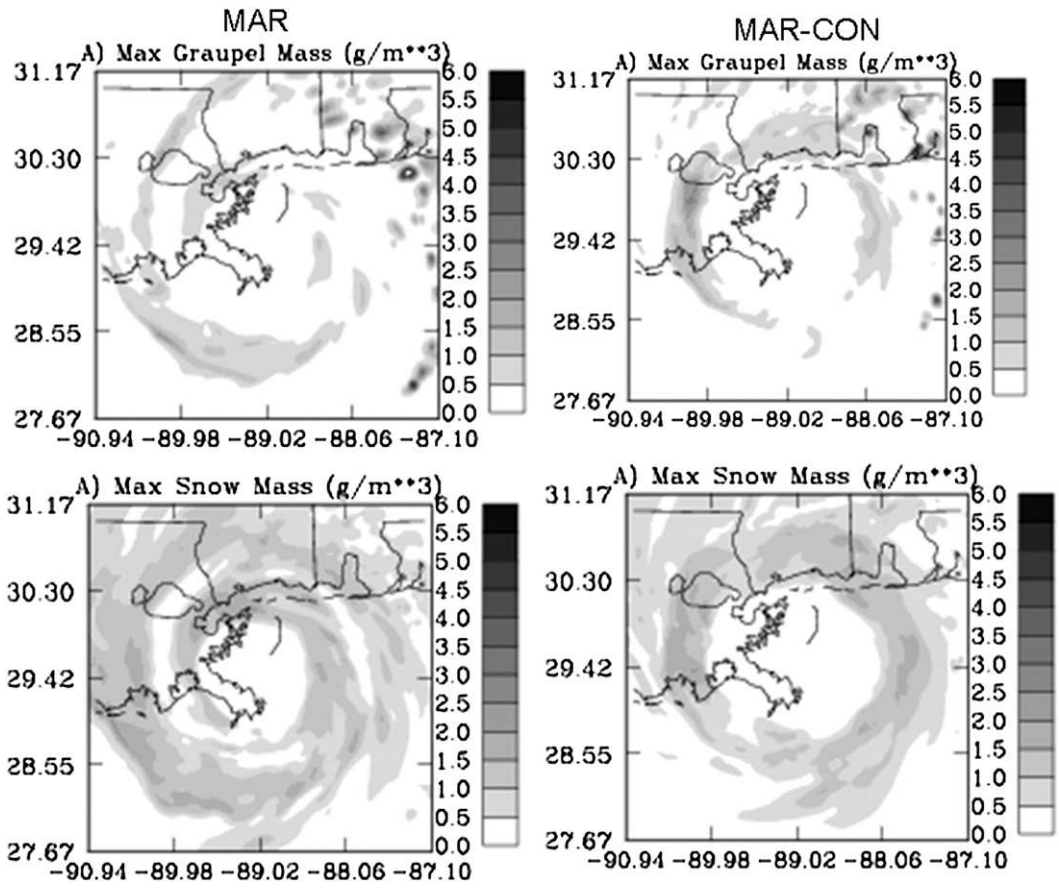

FIG. 11. As in Fig. 6, but for 0900 UTC 29 Aug.

TC weakening, which was the strongest when TC was located several hundred km offshore, remains significant during landfall. Continental aerosols change the spatial distribution of wind, precipitation, lightning, and other important parameters of landfalling TCs.

Figure 14 shows the LPI during the same time instances as in Fig. 13. One can see significant lightning intensity over the land, especially in MAR-CON. This agrees with observations of lightning during landfall (Shao et al. 2005). We attribute this effect to higher aerosol concentration in MAR-CON, which fosters the lightning formation.

4. Discussion and conclusions

a. The main results

For the first time tropical cyclone evolution was calculated using explicit (nonparameterized) spectral bin microphysics (SBM). Simulations with resolution of 3 km were made with the WRF/SBM. The evolution of Katrina was simulated during 72 h beginning after it had just bypassed Florida to 12 h after landfall. These simulations were used to investigate the effects of continental aerosols ingested into its circulation TC on TC structure and intensity. It is shown that at distances of a few hundred kilometers to the TC center aerosol concentration becomes similar to that over the land. It also was shown that some fraction of aerosols penetrated clouds in the eyewall, affecting their microphysical processes within the eyewall.

It is shown that continental aerosols invigorate convection (but largely at the TC periphery), which leads to TC weakening. Maximum TC weakening took place ~20 h before landfall, just after the TC intensity reached its maximum. The minimum pressure increased by ~15 hPa and maximum velocity decreased by about 15 m s^{-1}. However, the difference in the intensities remains significant even during the TC landfall. Thus, the results indicate that there is another (in addition to decrease in the surface fluxes) mechanism of weakening of TCs approaching the land. This mechanism is related to effects of continental aerosols involved into the TC circulation.

A scheme of the aerosol-induced TC weakening mechanism is illustrated in Fig. 15. The aerosol-induced

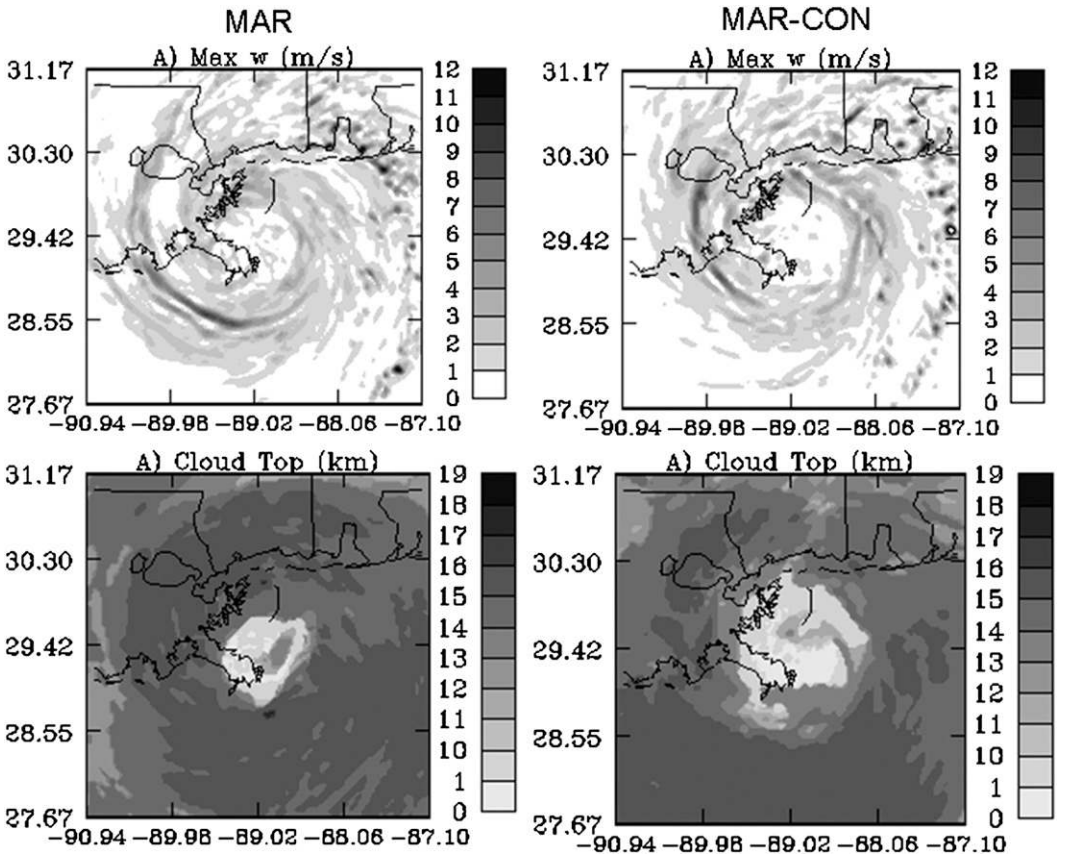

FIG. 12. As in Fig. 7, but for 0900 UTC 29 Aug.

intensification of convection leads to (a) an increase in w at TC periphery, causing mass updraft increases at the periphery with a smaller amount of air mass and water vapor penetrating to the central part of the TC; (b) extra convective heating at the periphery lowering the surface pressure at the TC periphery, decreasing the horizontal pressure gradient; and (c) competition between two zones of convection (TC eye and at TC periphery). Compensation downdrafts caused by convection at TC periphery also tend to damp the convection in the TC eye. As a result of the interaction between the radial circulations caused by the two convective zones, compensating downdrafts increase between these zones (at radii between 30–50 and ~100–150 km), as demonstrated by Khain et al. (2008a). The scheme shown in Fig. 15 agrees well with results of Saharan dust effects of TC intensity reported by Zhang et al. (2009). They found that convection in TC rainbands was negatively correlated with that in the eyewall in all simulations. The results agree well with recent observations by Jenkins et al. (2008) and Jenkins and Pratt (2008).

The aerosol effects on TC intensity obtained in the present study turn out to be stronger than those reported by Rosenfeld et al. (2007) and Khain et al. (2008a). We attribute this difference to the utilization of SBM that accurately describes cloud dynamics and microphysics (Khain and Lynn 2009; Khain et al. 2009). For instance, the convection invigoration and increase in cloud top at the TC periphery (accompanied by intensification of lightning) were observed in Hurricanes Katrina and Rita when they were located in the Gulf of Mexico (see Khain et al. 2008a for more detail). At the same time simulations with low aerosol concentration everywhere as well as simulations with bulk-convective parameterizations (Fierro et al. 2007) do not reveal these features. In the present study, the aerosol-induced transition from lightning within eyewall to the lightning at the TC periphery is simulated. This transition resembles well that observed in Hurricane Katrina during its approach to the land. (Katrina reached its maximum intensity around 1800 UTC 28 August and weakened as it approached land). The inner core of Katrina had collapsed during this period, and the storm became a very broad hurricane with close to 100-kt (51.44 m s^{-1}) winds extending almost 100 km from the storm center. This broadening and weakening during the last 6–8 h before landfall has

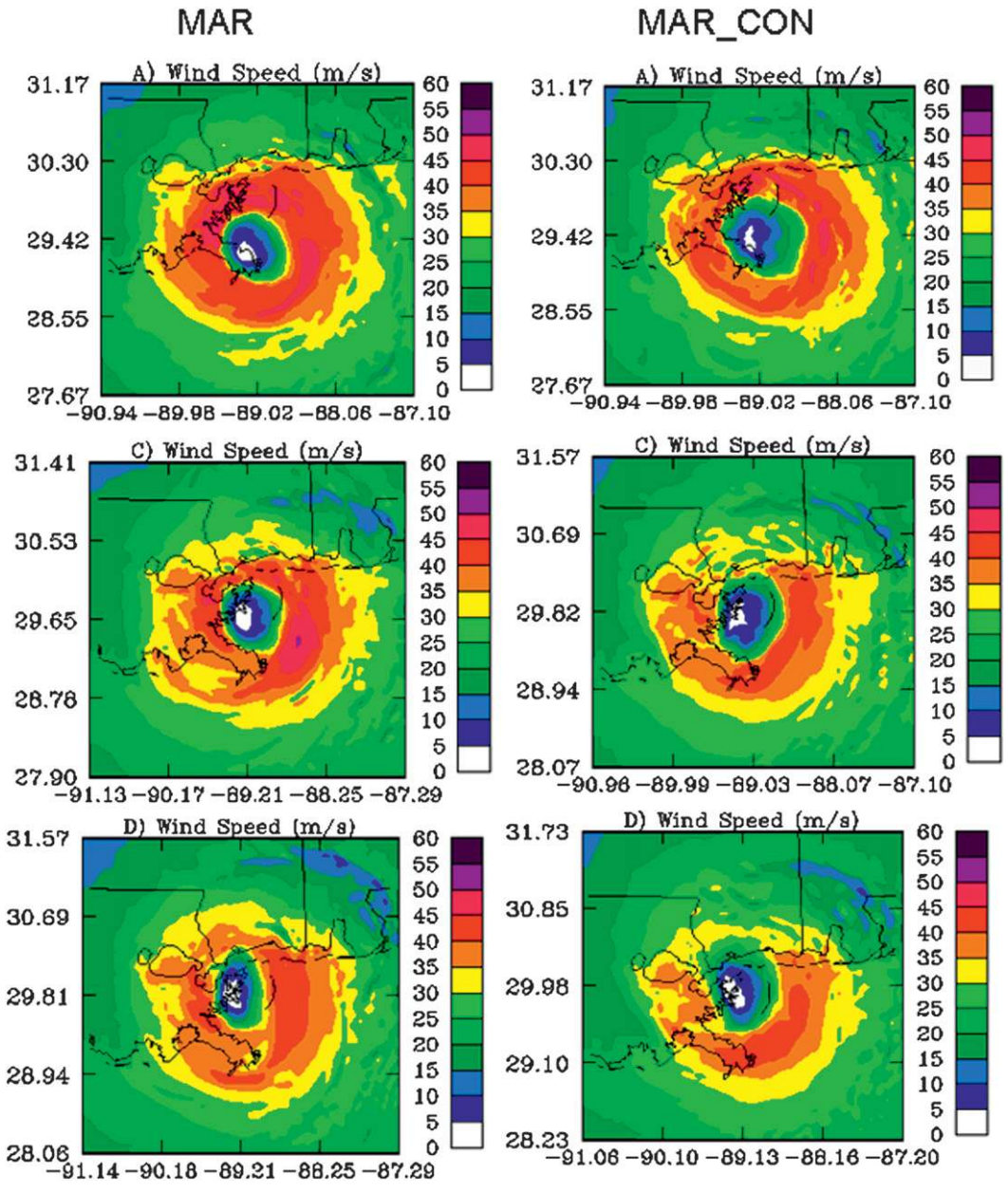

FIG. 13. The fields of the maximum wind speeds in (left) MAR and (right) MAR_CON at 0900, 1100, and 1200 UTC 29 Aug.

been difficult to capture in other simulations at NCAR and it can be speculated that aerosol effects played a role that has not been accounted for up to now. For instance, the eye radius and the radius of maximum winds during TC landfall were significantly larger in case aerosol effects were taken into account (see Figs. 11–14). It should be stressed that the weakening and the inner core collapsing was simulated in spite of the fact that the SST maximum was located near the coastal line, and no TC weakening caused by the TC–ocean interaction was taken into account. The structure of TC cloudiness in the simulation accounting for the effects of continental aerosol (MAR-CON) seems to be much more realistic than in the case that ignores the effects of continental aerosols (MAR).

Note that these results concerning deep maritime cloud response to aerosols agree qualitatively and even quantitatively with those obtained using high-resolution simulations (350 m × 125 m) using the Hebrew University Cloud model with SBM (Khain et al. 2008a). However, an increase in the WRF-SBM resolution is very desirable

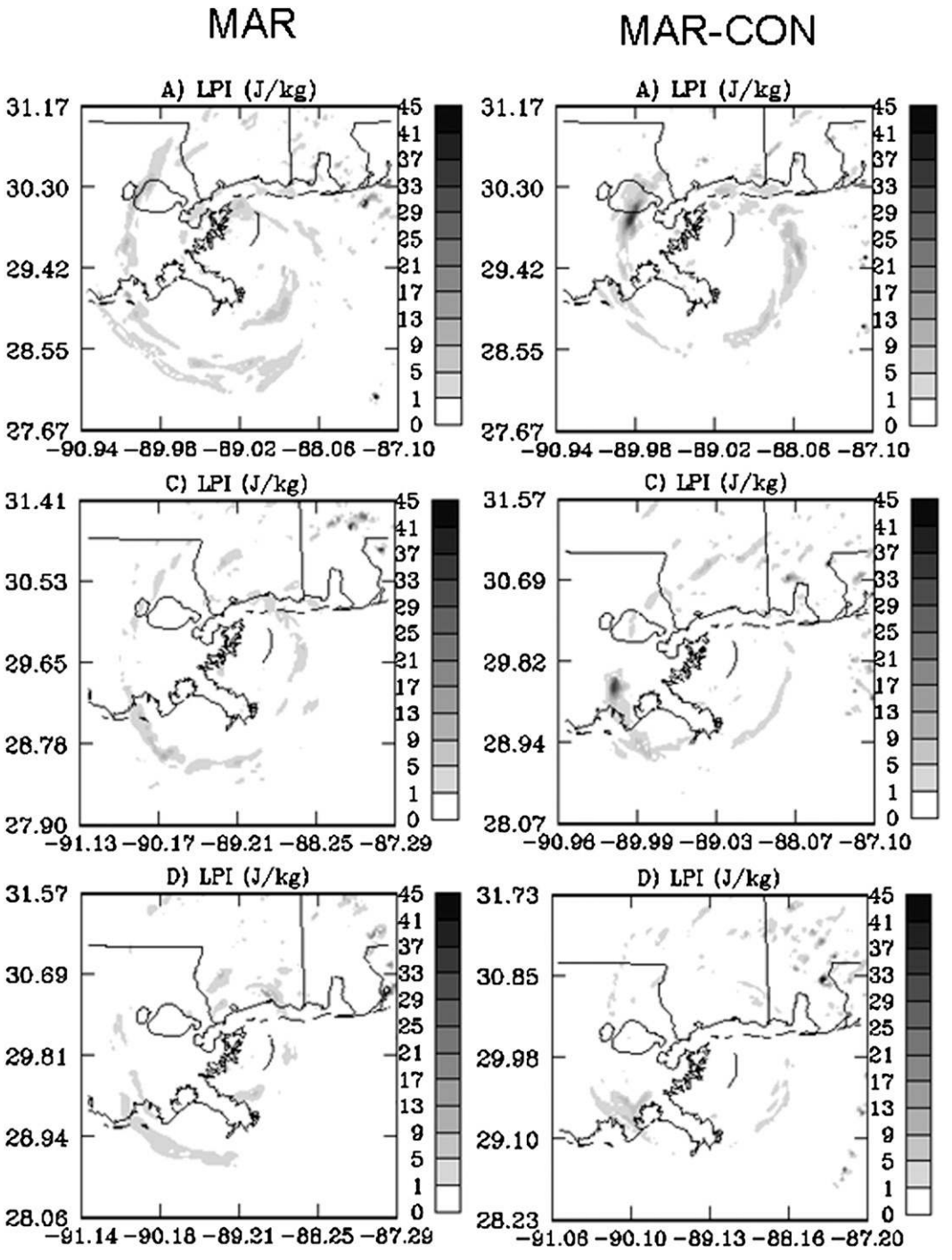

FIG. 14. As in Fig. 13, but for LPI.

to better resolve single clouds. It is especially important for a description of clouds at the TC periphery.

b. Necessary improvements

In spite of the substantial effects of aerosols on TC structure and intensity shown in the present study, we suppose that the further model improvements are required. First, the resolution used is not high enough to resolve all clouds at cloud periphery, which is very important to describe convective invigoration at the TC periphery properly. Higher resolution is required also to describe convective clouds in the TC eyewall.

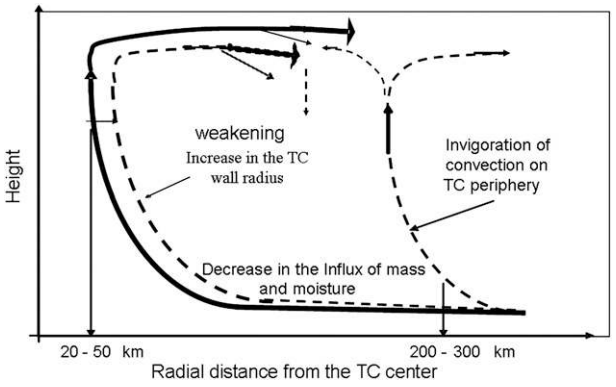

FIG. 15. A scheme of aerosol effects on the TC structure leading to TC weakening (see text for detail).

Second, the possible effects of sea spray on cloud microphysics were not taken into account. Sea spray forming at high winds produces many giant CCN that can (at least partially) prevent convective invigoration in the eyewall observed in the present study. As a result, convection invigoration should likely take place largely at the TC periphery, which will increase effects of continental aerosols on TC intensity. The aerosol effects found may be underestimated in the present study because of utilization of crude resolution of the reanalysis data. A TC of higher intensity could ingest more aerosols into its circulation. The scheme of TC assimilation should be included into the model. Finally, the size of the finest grid should be significantly increased. The utilization of the 400 km $\times$ 400 km fine grid precluded the additional intensification of the rainband at distances larger than 200 km from the TC center. It is quite possible that outer rings would be simulated beyond the radius of the present grid, each of which could undergo invigoration because of aerosol penetration.

c. *Perspective of utilization of the TC models with spectral bin microphysics*

The application of the explicit spectral bin microphysics in the TC models allows one to reproduce the fine microphysical structure of clouds in TCs and to take into account mechanisms and processes that affect cloud microphysics and dynamics. The SBM can allow explicit treatment of sea spray and its effect on surface fluxes as well as on cloud microphysics and precipitation because SBM describes explicitly evolution (evaporation, differential settling, collisions, etc.) of drop size distribution of sea spray during droplet ascent in the boundary layer to cloud base. Hence, the SBM is an ideal tool allowing improvement description of TC–ocean interaction. The TC models with SBM coupled with the ocean can be the basis for TC models of the next generation. Because TC intensity, structure, and precipitation depend on latent heat release determined by microphysical processes, the utilization of TC models with explicit SBM seems to open the way to improve prediction of TC intensity, wind, and precipitation and lightning of landfalling hurricanes. Many studies have focused on reproducing the rapid intensification but not on the collapse of the inner core and subsequent weakening as the storm approached the coast. The simulations with the SBM allowed reproduction of this effect. The utilization of TCs with explicit microphysics will allow simulation of TC genesis taking into account effects of Saharan dust. As shown by Zhang et al. (2007, 2009) and Jenkins et al. (2008), this effect may be quite significant. The utilization of explicit microphysics also allows investigation of the possibility of mitigating TC intensity by seeding clouds at the TC periphery with small aerosol particles, as discussed by Rosenfeld et al. (2007), Cotton et al. (2007), and Khain et al. (2008a).

In conclusion, we would like to stress that the simulations of the current version of the TC model with spectral bin microphysics for 72 h were performed using a standard PC cluster with eight processors and a limited memory volume. The simulations require 10 days of computer time. It means that WRF with spectral bin microphysics can be used for scientific purposes using computers available in most scientific centers.

Acknowledgments. The study was supported by the Israel Science Foundation (Grant 140/07) and scientific project Hurricane Aerosol and Microphysics Program (HAMP) (Project FY2008-06-16). The authors express their deep gratitude to H. Zvi Kruglyak for help with computer problems.

REFERENCES

Andreae, M. O., D. Rosenfeld, P. Artaxo, A. A. Costa, G. P. Frank, K. M. Longlo, and M. A. F. Silva-Dias, 2004: Smoking rain clouds over the Amazon. *Science,* **303,** 1337–1342.

Anthes, R. A., 1982: *Tropical Cyclones—Their Evolution, Structure, and Effects. Meteor. Monogr.,* No. 41, Amer. Meteor. Soc., 208 pp.

Arakawa, A., and W. H. Shubert, 1974: Interaction of a cumulus cloud ensemble with the large-scale environment, Part I. *J. Atmos. Sci.,* **31,** 674–701.

Bender, M. A., and I. Ginis, 2000: Real-case simulations of hurricane–ocean interaction using a high-resolution coupled model: Effects on hurricane intensity. *Mon. Wea. Rev.,* **128,** 917–946.

——, ——, R. Tuleya, B. Thomas, and T. Marchok, 2007: The operational GFDL coupled hurricane–ocean prediction system and a summary of its performance. *Mon. Wea. Rev.,* **135,** 3965–3989.

Betz, H. D., U. Schumann, and P. Laroche, Eds., 2008: *Lightning: Principles, Instruments and Applications—Review of Modern Lighting Research.* Springer, 641 pp.

Black, M. L., R. W. Burpee, and F. D. Marks Jr., 1996: Vertical motion characteristics of tropical cyclones determined with airborne Doppler radar velocities. *J. Atmos. Sci.,* **53,** 1887–1909.

Black, R. A., and J. Hallett, 1986: Observations of the distribution of ice in hurricanes. *J. Atmos. Sci.,* **43,** 802–822.

——, and ——, 1999: Electrification of the hurricane. *J. Atmos. Sci.,* **56,** 2004–2028.

Bott, A., 1998: A flux method for the numerical solution of the stochastic collection equation. *J. Atmos. Sci.,* **55,** 2284–2293.

Cecil, D. J., and S. W. Nebitt, 2002: Reflectivity, ice scattering, and lightning characteristics of hurricane eyewalls and rainbands. Part II: Intercomparison of observations. *Mon. Wea. Rev.,* **130,** 785–801.

——, E. J. Zipser, and S. W. Nebitt, 2002: Reflectivity, ice scattering, and lightning characteristics of hurricane eyewalls and rainbands. Part I: Quantitative description. *Mon. Wea. Rev.,* **130,** 769–784.

Chronis, T., E. Williams, E. Anagnostou, and W. Petersen, 2007: African lightning: Indicator of tropical Atlantic cyclone formation. *Eos, Trans. Amer. Geophys. Union,* **88,** doi:10.1029/2007EO400001.

Cotton, W. R., H. Zhang, G. M. McFarquhar, and S. M. Saleeby, 2007: Should we consider polluting hurricanes to reduce their intensity? *J. Wea. Modif.,* **39,** 70–73.

Demetriades, N. W. S., and R. L. Holle, 2006: Long-range lightning nowcasting applications for tropical cyclones. Preprints, *Conf. on Meteorology Application of Lightning Data,* Atlanta, GA, Amer. Meteor. Soc., P2.15. [Available online at http://ams.confex.com/ams/pdfpapers/99183.pdf.]

Dudhia, J., 1993: A nonhydrostatic version of the Penn State/NCAR mesoscale model: Validation tests and simulation of an Atlantic cyclone and cold front. *Mon. Wea. Rev.,* **121,** 1493–1513.

Emanuel, K., 2005: *Divine Wind: The History and Science of Hurricanes*. Oxford University Press, 296 pp.

Falkovich, A. I., A. P. Khain, and I. Ginis, 1995: Motion and evolution of binary tropical cyclones in a coupled atmosphere–ocean numerical model. *Mon. Wea. Rev.,* **123,** 1345–1363.

Fan, J., M. Ovtchinnikov, J. Comstock, S. McFarlane, and A. Khain, 2009: Ice formation in Arctic mixed-phase clouds: Insights from a 3-D cloud-resolving model with size-resolved aerosol and cloud microphysics. *J. Geophys. Res.,* **114,** D04205, doi:10.1029/2008JD010782.

Ferrier, B. S., 2005: An efficient mixed-phase cloud and precipitation scheme for use in operational NWP models. *Proc. Amer. Geophys. Union Spring Meeting,* New Orleans, LA, Amer. Geophys. Union, A42A-02.

Fierro, A. O., L. Leslie, E. Mansell, J. Straka, D. MacGorman, and C. Ziegler, 2007: A high-resolution simulation of microphysics and electrification in an idealized hurricane-like vortex. *Meteor. Atmos. Phys.,* **98,** 13–33, doi:10.1007/s00703-006-0237-0.

Hallett, J., and S. C. Mossop, 1974: Production of secondary ice particles during the riming process. *Nature,* **249,** 26–28.

Iguchi, T., T. Nakajima, A. Khain, K. Saito, T. Takemura, and K. Suzuki, 2008: Modeling the influence of aerosols on cloud microphysical properties in the East Asia region using a mesoscale model coupled with a bin-based cloud microphysics scheme. *J. Geophys. Res.,* **113,** D14215, doi:10.1029/2007JD009774.

Jenkins, G. S., and A. Pratt, 2008: Saharan dust, lightning and tropical cyclones in the eastern tropical Atlantic during NAMMA-06. *Geophys. Res. Lett.,* **35,** L12804, doi:10.1029/2008GL033979.

——, A. S. Pratt, and A. Heymsfield, 2008: Possible linkages between Saharan dust and tropical cyclone rain band invigoration in the eastern Atlantic during NAMMA-06. *Geophys. Res. Lett.,* **35,** L08815, doi:10.1029/2008GL034072.

Jorgensen, D. P., and M. A. LeMone, 1989: Vertical velocity characteristics of oceanic convection. *J. Atmos. Sci.,* **46,** 621–640.

——, E. J. Zipser, and M. A. LeMone, 1985: Vertical motions in intense hurricanes. *J. Atmos. Sci.,* **42,** 839–856.

Khain, A. P., 1984: *Mathematical Modeling of Tropical Cyclones*. Gidrometeoizdat, 247 pp.

——, 2009: Notes on state-of-the-art investigations of aerosol effects on precipitation: A critical review. *Environ. Res. Lett.,* **4,** 015004, doi:10.1088/1748-9326/4/1/015004.

——, and G. G. Sutyrin, 1983: *Tropical Cyclones and Their Interaction with the Ocean*. Gidrometeoizdat, 241 pp.

——, and E. A. Agrenich, 1987: Possible effect of atmospheric humidity and radiation heating of dusty air on tropical cyclone development. *Proc. Inst. Exp. Meteor.,* **42,** 77–80.

——, and I. Sednev, 1996: Simulation of precipitation formation in the eastern Mediterranean coastal zone using a spectral microphysics cloud ensemble model. *Atmos. Res.,* **43,** 77–110.

——, and B. Lynn, 2009: Simulation of a supercell storm in clean and dirty atmosphere using weather research and forecast model with spectral bin microphysics. *J. Geophys. Res.,* **114,** D19209, doi:10.1029/2009JD011827.

——, M. Ovtchinnikov, M. Pinsky, A. Pokrovsky, and H. Krugliak, 2000: Notes on the state-of-the-art numerical modeling of cloud microphysics. *Atmos. Res.,* **55,** 159–224.

——, M. B. Pinsky, M. Shapiro, and A. Pokrovsky, 2001a: Collision rate of small graupel and water drops. *J. Atmos. Sci.,* **58,** 2571–2595.

——, D. Rosenfeld, and A. Pokrovsky, 2001b: Simulating convective clouds with sustained supercooled liquid water down to −37.5°C using a spectral microphysics model. *Geophys. Res. Lett.,* **28,** 3887–3890.

——, A. Pokrovsky, M. Pinsky, A. Seifert, and V. Phillips, 2004: Simulation of effects of atmospheric aerosols on deep turbulent convective clouds using a spectral microphysics mixed-phase cumulus cloud model. Part I: Model description and possible applications. *J. Atmos. Sci.,* **61,** 2963–2982.

——, D. Rosenfeld, and A. Pokrovsky, 2005: Aerosol impact on the dynamics and microphysics of deep convective clouds. *Quart. J. Roy. Meteor. Soc.,* **131,** 2639–2663.

——, N. Cohen, B. Lynn, and A. Pokrovsky, 2008a: Possible aerosol effects on lightning activity and structure of hurricanes. *J. Atmos. Sci.,* **65,** 3652–3677.

——, N. BenMoshe, and A. Pokrovsky, 2008b: Factors determining the impact of aerosols on surface precipitation from clouds: An attempt at classification. *J. Atmos. Sci.,* **65,** 1721–1748.

——, L. R. Leung, B. Lynn, and S. Ghan, 2009: Effects of aerosols on the dynamics and microphysics of squall lines simulated by spectral bin and bulk parameterization schemes. *J. Geophys. Res.,* **114,** D22203, doi:10.1029/2009JD011902.

Koren, I., Y. J. Kaufman, D. Rosenfeld, L. A. Remer, and Y. Rudich, 2005: Aerosol invigoration and restructuring of Atlantic convective clouds. *Geophys. Res. Lett.,* **32,** L14828, doi:10.1029/2005GL023187.

Kurihara, Y., 1973: A scheme of moist convective adjustment. *Mon. Wea. Rev.,* **101,** 547–553.

Lee, S. S., L. J. Donner, V. T. J. Phillips, and Y. Ming, 2008: The dependence of aerosol effects on clouds and precipitation on cloud-system organization, shear and stability. *J. Geophys. Res.,* **113,** D16202, doi:10.1029/2007JD009224.

Levin, Z., and W. R. Cotton, 2009: *Aerosol Pollution Impact on Precipitation: A Scientific Review*. Springer, 386 pp.

Lhermitte, R. M., and P. Krehbiel, 1979: Doppler radar and radio observations of thunderstorms. *IEEE Trans. Geosci. Electron.,* **17,** 162–171.

Li, X., W.-K. Tao, A. P. Khain, J. Simpson, and D. E. Johnson, 2009a: Sensitivity of a cloud-resolving model to bulk and explicit bin microphysical schemes. Part I: Comparisons. *J. Atmos. Sci.,* **66,** 3–21.

——, ——, ——, ——, and ——, 2009b: Sensitivity of a cloud-resolving model to bulk and explicit bin microphysical schemes. Part II: Cloud microphysics and storm dynamics interactions. *J. Atmos. Sci.,* **66,** 22–40.

Lynn, B., and A. Khain, 2007: Utilization of spectral bin microphysics and bulk parameterization schemes to simulate the cloud structure and precipitation in a mesoscale rain event. *J. Geophys. Res.,* **112,** D22205, doi:10.1029/2007JD008475.

——, ——, J. Dudhia, D. Rosenfeld, A. Pokrovsky, and A. Seifert, 2005a: Spectral (bin) microphysics coupled with a mesoscale model (MM5). Part I: Model description and first results. *Mon. Wea. Rev.,* **133,** 44–58.

——, ——, ——, ——, ——, and ——, 2005b: Spectral (bin) microphysics coupled with a mesoscale model (MM5). Part II: Simulation of a CAPE rain event with squall line. *Mon. Wea. Rev.,* **133,** 59–71.

Lyons, W. A., and C. S. Keen, 1994: Observations of lightning in convective supercells within tropical storms and hurricanes. *Mon. Wea. Rev.,* **122,** 1897–1916.

McFarquhar, G., and R. A. Black, 2004: Observations of particle size and phase in tropical cyclones: Implications for mesoscale modeling of microphysical processes. *J. Atmos. Sci.,* **61,** 422–439.

Meyers, M. P., P. J. DeMott, and W. R. Cotton, 1992: New primary ice-nucleation parameterizations in an explicit cloud model. *J. Appl. Meteor.,* **31,** 708–721.

Molinari, J., P. K. Moore, V. P. Idone, R. W. Henderson, and A. B. Saljoughy, 1994: Cloud-to-ground lightning in Hurricane Andrew. *J. Geophys. Res.,* **99,** 16 665–16 676.

——, ——, and ——, 1999: Convective structure of hurricanes as revealed by lightning locations. *Mon. Wea. Rev.,* **127,** 520–534.

Orville, R. E., and J. M. Coyne, 1999: Cloud-to-ground lightning in tropical cyclones (1986–1996). Preprints, *23rd Conf. on Hurricanes and Tropical Meteorology,* Dallas, TX, Amer. Meteor. Soc., 194–198.

Pielke, R. A., and Coauthors, 1992: A comprehensive meteorological modeling system—RAMS. *Meteor. Atmos. Phys.,* **49,** 69–91.

Pinsky, M., and A. P. Khain, 2002: Effects of in-cloud nucleation and turbulence on droplet spectrum formation in cumulus clouds. *Quart. J. Roy. Meteor. Soc.,* **128,** 501–533.

——, ——, and M. Shapiro, 2001: Collision efficiency of drops in a wide range of Reynolds numbers: Effects of pressure on spectrum evolution. *J. Atmos. Sci.,* **58,** 742–764.

Price, C., M. Asfur, and Y. Yair, 2009: Maximum hurricane intensity preceded by increase in lightning frequency. *Nature Geosci.,* **2,** 329–332, doi:10.1038/NGEO477.

Pruppacher, H. R., 1995: A new look at homogeneous ice nucleation in supercooled water drops. *J. Atmos. Sci.,* **52,** 1924–1933.

——, and J. D. Klett, 1997: *Microphysics of Clouds and Precipitation*. 2nd ed. Oxford University Press, 963 pp.

Rodgers, E., J. Weinman, H. Pierce, and W. Olson, 2000: Tropical cyclone lightning distribution and its relationship to convection and intensity change. Preprints, *24th Conf. on Hurricanes and Tropical Meteorology,* Ft. Lauderdale, FL, Amer. Meteor. Soc., 537–541.

Rosenfeld, D., A. Khain, B. Lynn, and W. L. Woodley, 2007: Simulation of hurricane response to suppression of warm rain by submicron aerosols. *Atmos. Chem. Phys. Discuss.,* **7,** 5647–5674.

——, U. Lohmann, G. B. Raga, C. D. O'Dowd, M. Kulmala, S. Fuzzi, A. Reissell, and M. O. Andreae, 2008: Flood or drought: How do aerosols affect precipitation? *Science,* **321,** 1309–1313.

Saleeby, S. M., and W. R. Cotton, 2004: A large-droplet mode and prognostic number concentration of cloud droplets in the Colorado State University Regional Atmospheric Modeling System (RAMS). Part I: Module descriptions and supercell test simulations. *J. Appl. Meteor.,* **43,** 182–195.

——, and ——, 2008: A binned approach to cloud droplet riming implemented in a bulk microphysics model. *J. Appl. Meteor. Climatol.,* **47,** 694–703.

Saunders, C. P. R., 1993: A review of thunderstorm electrification processes. *J. Appl. Meteor.,* **32,** 642–655.

Segal, Y., and A. Khain, 2006: Dependence of droplet concentration on aerosol conditions in different cloud types: Application to droplet concentration parameterization of aerosol conditions. *J. Geophys. Res.,* **111,** doi:10.1029/2005JD006561.

——, M. Pinsky, A. Khain, and C. Erlick, 2003: Thermodynamic factors influencing bimodal spectrum formation in cumulus clouds. *Atmos. Res.,* **66,** 43–64.

Seifert, A., and K. Beheng, 2006: A two-moment cloud microphysics parameterization for mixed-phase clouds. Part 1: Model description. *Meteor. Atmos. Phys.,* **92,** 45–66.

——, A. Khain, U. Blahak, and K. Beheng, 2005: Possible effects of collisional breakup on mixed-phase deep convection simulated by a spectral (bin) cloud model. *J. Atmos. Sci.,* **62,** 1917–1931.

Shao, X.-M., and Coauthors, 2005: Katrina and Rita were lit up with lightning. *Eos, Trans. Amer. Geophys. Union,* **86,** doi:10.1029/2005EO420004.

Sherwood, S. C., V. Phillips, and J. S. Wettlaufer, 2006: Small ice crystals and the climatology of lightning. *Geophys. Res. Lett.,* **33,** L05804, doi:10.1029/2005GL025242.

Simpson, R. H., and J. S. Malkus, 1964: Experiments in hurricane modification. *Sci. Amer.,* **211,** 27–37.

Skamarock, W. C., J. B. Klemp, J. Dudhia, D. O. Gill, D. M. Barker, W. Wang, and J. G. Powers, 2005: A description of the Advanced Research WRF version 2. NCAR Tech Note NCAR-468+STR, 88 pp.

Takahashi, T., 1978: Riming electrification as a charge generation mechanism in thunderstorms. *J. Atmos. Sci.,* **35,** 1536–1548.

Tao, W.-K., X. Li, A. Khain, T. Matsui, S. Lang, and J. Simpson, 2007: The role of atmospheric aerosol concentration on deep convective precipitation: Cloud-resolving model simulations. *J. Geophys. Res.,* **112,** D24S18, doi:10.1029/2007JD008728.

Thompson, G., P. R. Field, W. D. Hall, and R. Rasmussen, 2006: A new bulk microphysical parameterization for WRF (& MM5). *Proc. Seventh Weather Research and Forecasting User's Workshop,* Boulder, CO, NCAR, 1–11. [Available online at http://www.mmm.ucar.edu/wrf/users/workshops/WS2006/abstracts/Session05/5_3_Thompson.pdf.]

Tzivion, S., G. Feingold, and Z. Levin, 1989: The evolution of raindrop spectra. Part II. Collisional collection/breakup and evaporation in a rainshaft. *J. Atmos. Sci.,* **46,** 3312–3327.

Vali, G., 1975: Remarks on the mechanism of atmospheric ice nucleation. *Proc. Eighth Int. Conf. on Nucleation,* Leningrad, U.S.S.R., Gidrometeoizdat, 265–269.

——, 1994: Freezing rate due to heterogeneous nucleation. *J. Atmos. Sci.,* **51,** 1843–1856.

Wang, C., 2005: A modeling study of the response of tropical deep convection to the increase of cloud condensational nuclei concentration: 1. Dynamics and microphysics. *J. Geophys. Res.,* **110,** D21211, doi:10.1029/2004JD005720.

Wiens, K. C., S. A. Rutledge, and S. A. Tessendorf, 2005: The 29 June 2000 supercell observed during STEPS. Part 2: Lightning and charge structure. *J. Atmos. Sci.,* **62,** 4151–4177.

Williams, E., and G. Satori, 2004: Lightning, thermodynamic and hydrological comparison of the two tropical continental chimneys. *J. Atmos. Solar-Terr. Phys.,* **66,** 1213–1231.

——, V. Mushtak, D. Rosenfeld, S. Goodman, and D. Boccippio, 2005: Thermodynamic conditions favorable to superlative thunderstorm updraft, mixed phase microphysics and lightning flash rate. *Atmos. Res.,* **76,** 288–306.

Willoughby, H. E., D. P. Jorgensen, R. A. Black, and S. L. Rosenthal, 1985: Project STORMFURY: A scientific chronicle, 1962–1983. *Bull. Amer. Meteor. Soc.,* **66,** 505–514.

Yair, Y., B. Lynn, C. Price, V. Kotroni, K. Lagouvardos, E. Morin, A. Mugnai, and M. Llasat, 2009: Predicting the potential for lightning activity in Mediterranean storms based on the WRF model dynamic and microphysical fields. *J. Geophys. Res.,* doi:10.1029/2008JD010868, in press.

Zhang, H., G. M. McFarquhar, S. M. Saleeby, and W. R. Cotton, 2007: Impacts of Saharan dust as CCN on the evolution of an idealized tropical cyclone. *Geophys. Res. Lett.,* **34,** L14812, doi:10.1029/2007GL029876.

——, ——, W. R. Cotton, and Y. Deng, 2009: Direct and indirect impacts of Saharan dust acting as cloud condensation nuclei on tropical cyclone eyewall development. *Geophys. Res. Lett.,* **36,** L06802, doi:10.1029/2009GL037276.